ResearchGate

See discussions, stats, and author profiles for this publication at: https://www.researchgate.net/publication/23807829

Raman Scattering from Nonequilibrium Molecular Conduction Junctions

ARTICLE *in* NANO LETTERS · FEBRUARY 2009

Impact Factor: 13.59 · DOI: 10.1021/nl803313f · Source: PubMed

CITATIONS
35

READS
23

3 AUTHORS, INCLUDING:

Michael Galperin
University of California, San Diego

82 PUBLICATIONS **2,540** CITATIONS

SEE PROFILE

Mark A. Ratner
Northwestern University

906 PUBLICATIONS **42,483** CITATIONS

SEE PROFILE

Available from: Michael Galperin
Retrieved on: 30 January 2016

NANO LETTERS

Subscriber access provided by TEL AVIV UNIV (AO)

Letter

Raman Scattering from Nonequilibrium Molecular Conduction Junctions

Michael Galperin, Mark A. Ratner, and Abraham Nitzan

Nano Lett., **2009**, 9 (2), 758-762• DOI: 10.1021/nl803313f • Publication Date (Web): 21 January 2009

Downloaded from http://pubs.acs.org on February 18, 2009

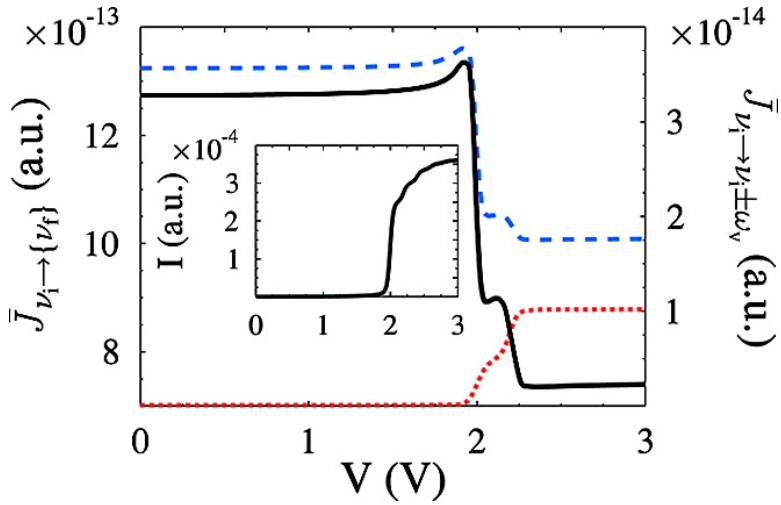

More About This Article

Additional resources and features associated with this article are available within the HTML version:

- Supporting Information
- Access to high resolution figures
- Links to articles and content related to this article
- Copyright permission to reproduce figures and/or text from this article

View the Full Text HTML

ACS Publications
High quality. High impact.

Nano Letters is published by the American Chemical Society. 1155 Sixteenth Street N.W., Washington, DC 20036

NANO LETTERS

2009
Vol. 9, No. 2
758-762

Raman Scattering from Nonequilibrium Molecular Conduction Junctions

Michael Galperin,*,† Mark A. Ratner,‡ and Abraham Nitzan§

Department of Chemistry & Biochemistry, University of California at San Diego, La Jolla, California 92093, Department of Chemistry, Northwestern University, Evanston Illinois 60208, and School of Chemistry, The Sackler Faculty of Science, Tel Aviv University, Tel Aviv 69978, Israel

Received November 3, 2008; Revised Manuscript Received December 26, 2008

ABSTRACT

Raman scattering is a potentially important probe of structure, dynamics, and thermal properties of single-molecule conduction junctions. We combine a nonequilibrium Green's function description of the junction with a generalized scattering theory of the Raman process, which provides the first theoretical description of Raman scattering from such systems. The voltage dependence of the Raman flux shows a characteristic behavior at the conductance threshold resulting from (a) partial populations in the ground and excited molecular levels that give rise to two scattering pathways as well as interference between them and (b) junction heating that affects the Raman intensities. Comparing "effective temperatures" obtained from Raman scattering and heat balance serves to establish the integrity of this concept for nonequilibrium junctions.

The interaction of molecular conduction junctions with the radiation field has been explored as a way for characterizing and controlling their operation.[1,2] In particular, optical switching of such junctions was demonstrated[3−5] and studied theoretically[6,7] Laser control of junction operation and their noise properties was studied theoretically.[8−14] The effect of illumination on the conduction properties of atomic size contacts was studied experimentally,[15] and implications for molecular junctions were considered theoretically.[16]

Surface-enhanced Raman and resonance Raman spectroscopies (SERS and SERRS)[17,18] have become important diagnostic tools for many science applications. The observation of single-molecule SERS and SERRS[19,20] indicates that the signal is often dominated by molecules adsorbed at particular "hot spots". Single-molecule transport junctions, molecules connecting two metal leads, whose electrical transport properties are under intensive study,[21] have structures similar (e.g., ref 22) to models used for such hot spots. Monitoring SERS and SERRS together with electronic transport in such junctions[23−26] will provide new diagnostic tools for molecular electronics and requires a suitable theoretical description of the optical response of nonequilibrium open nanosystems. Here we outline a first theoretical treatment of Raman scattering from nonequilibrium molecular conduction junctions (for the full theoretical treatment see ref 27) and describe its main experimental implications.

* Corresponding author, migalperin@ucsd.edu.
† University of California at San Diego.
‡ Northwestern University.
§ Tel Aviv University.

The molecule is modeled as a two-electronic-levels system interacting with a molecular vibration, with the continuum electronic manifolds of the electrodes (with an applied voltage across them) and with the radiation field. The theoretical treatment needs to account for nonequilibrium nature of the electronic transport together with the scattering of photons off of the molecule.

We focus on response to the *local* electromagnetic field, which is assumed independent of the imposed potential bias and therefore amenable to independent calculation. We employ a generalized spinless model,[28] comprising a molecule coupled to two metal leads (L and R) each in its own thermal equilibrium. The molecule is represented by its highest occupied and lowest unoccupied molecular orbitals, HOMO = 1 and LUMO = 2, with populations (n_1, n_2), respectively, that describe the ground (1,0) and lowest excited (0,1) molecular states, as well as positive (0,0) and negative (1,1) ion states. The Hamiltonian is $\hat{H} = \hat{H}_0 + \hat{V}^{(\mathrm{e-v})} + \hat{V}^{(\mathrm{et})} + \hat{V}^{(\mathrm{v-b})} + \hat{V}^{(\mathrm{e-h})} + \hat{V}_M^{(\mathrm{e-p})} + \hat{V}_{CT}^{(\mathrm{e-p})}$ with

$$\hat{H}_0 = \sum_{m=1,2} \varepsilon_m \hat{d}_m^\dagger \hat{d}_m + \omega_\upsilon \hat{b}_\upsilon^\dagger \hat{b}_\upsilon + \sum_{k\in L,R} \varepsilon_k \hat{c}_k^\dagger \hat{c}_k + \sum_\beta \omega_\beta \hat{b}_\beta^\dagger \hat{b}_\beta + \sum_{\alpha\in\{i,\{f\}\}} \nu_\alpha \hat{a}_\alpha^\dagger \hat{a}_\alpha \quad (1)$$

$$\hat{V}^{(\mathrm{e-v})} = \sum_{m=1,2} V_m^{(\mathrm{e-v})} \hat{Q}_\upsilon \hat{d}_m^\dagger \hat{d}_m \quad (2)$$

$$\hat{V}^{(\mathrm{et})} = \sum_{K=L,R} \sum_{k\in K;m} (V_{km}^{(\mathrm{et})} \hat{c}_k^\dagger \hat{d}_m + V_{mk}^{(\mathrm{et})} \hat{d}_m^\dagger \hat{c}_k) \quad (3)$$

10.1021/nl803313f CCC: $40.75 © 2009 American Chemical Society
Published on Web 01/21/2009

$$\hat{V}^{(\mathrm{v-b})} = \sum_{\beta} U_{\beta}^{(\mathrm{v-b})} \hat{Q}_{\nu} \hat{Q}_{\beta} \tag{4}$$

$$\hat{V}^{(\mathrm{e-h})} = \sum_{k_1 \neq k_2} (V_{k_1 k_2}^{(\mathrm{e-h})} \hat{D}^{\dagger} \hat{c}_{k_1}^{\dagger} \hat{c}_{k_2} + \mathrm{H.c}) \tag{5}$$

$$\hat{V}_{M}^{(\mathrm{e-p})} = \sum_{\alpha \in \{i,\{f\}\}} (U_{\alpha}^{(\mathrm{e-p})} \hat{D}^{\dagger} \hat{a}_{\alpha} + \overset{*}{U}_{\alpha}^{(\mathrm{e-p})} \hat{a}_{\alpha}^{\dagger} \hat{D}) \tag{6a}$$

$$\hat{V}_{CT}^{(\mathrm{e-p})} = \sum_{\alpha \in \{i,\{f\}\}} \sum_{k \in \{L,R\}} \sum_{m=1,2} (\hat{a}_{\alpha} + \hat{a}_{\alpha}^{\dagger})[V_{km,\alpha}^{(\mathrm{e-p})} \hat{D}_{km} + V_{mk,\alpha}^{(\mathrm{e-p})} \hat{D}_{mk}] \tag{6b}$$

$\hat{H}_0$ includes additively the Hamiltonians for the molecular electronic and vibrational subsystems, the metal electrons, and the radiation field. $\hat{d}_m^{\dagger}$ ($\hat{d}_m$) and $\hat{c}_k^{\dagger}$ ($\hat{c}_k$) create (annihilate) an electron in the molecular state m and in the lead state k of energies ε_m and ε_k, respectively. $\hat{b}_{\nu}^{\dagger}$ ($\hat{b}_{\nu}$) and $\hat{b}_{\beta}^{\dagger}$ ($\hat{b}_{\beta}$) create (annihilate) vibrational quanta in the molecular mode,ν, and the thermal bath mode, β, respectively. $\hat{a}_{\alpha}^{\dagger}$ ($\hat{a}_{\alpha}$) stands for creation (annihilation) operators of radiation field quanta. ω and ν denote frequencies of phonon and photon modes, respectively. Also $\hat{Q}_j \equiv \hat{b}_j + \hat{b}_j^{\dagger}$, $j = \nu, \beta$ are displacement operators for the molecular (ν) and thermal bath (β) vibrations, respectively. The corresponding momentum operators are $\hat{P}_j \equiv - i(\hat{b}_j - \hat{b}_j^{\dagger})$, $j = \nu, \beta$. $\hat{V}^{\mathrm{et}}$, $\hat{V}^{(\mathrm{e-h})}$, $\hat{V}^{(\mathrm{e-v})}$, and $\hat{V}^{(\mathrm{v-b})}$ are the couplings associated with electron transfer between molecule and leads, coupling of molecular excitation to electron−hole pairs in the leads, electron−molecular vibration interaction and coupling between the molecular vibration and the thermal bath, respectively. $\hat{V}_{\mathrm{M}}^{(\mathrm{e-p})}$ and $V_{\mathrm{CT}}^{(\mathrm{e-p})}$ are radiative coupling terms. The former is associated with the molecular transition, while the latter accounts for metal−molecule charge transfer (CT) transitions. $\hat{D} \equiv \hat{d}_1^{\dagger} \hat{d}_2$, $\hat{D}^{\dagger} \equiv \hat{d}_2^{\dagger} \hat{d}_1$ are the molecular polarization operators and similarly, $\hat{D}_{mk} \equiv \hat{d}_m^{\dagger} \hat{c}_k$, $\hat{D}_{km} \equiv \hat{c}_k^{\dagger} \hat{d}_m$ ($m = 1, 2$). Here and below we put $e = 1$, $\hbar = 1$, and $k_{\mathrm{B}} = 1$ for the electron charge and the Planck and Boltzmann constants, respectively. Note that in our formulation we use zero and one photon occupations of the relevant radiation field modes. Therefore the coupling amplitudes $U_{\alpha}^{(\mathrm{e-p})}$ and $V_{km,\alpha}^{(\mathrm{e-p})}$ reflect the intensity of the local electromagnetic field, including effects of plasmon excitations in the leads. Also, the vibronic coupling (2), a parallel shift in harmonic nuclear potential surfaces between different electronic states, is common in molecular spectroscopy but its applicability to Raman scattering is limited to near resonance situations. This makes our theory valid for resonance Raman scattering, although it can provide qualitative insight also for the off-resonance case. The model Hamiltonian $\hat{H}$ describes inelastic light scattering superimposed on inelastic electron tunneling in a biased molecular junction. The former will be treated in the lowest (fourth) order appropriate for Raman scattering. The latter has been under intense study in recent years,[29] mostly in the context of inelastic tunneling spectroscopy. Its handling follows our previous work[29,30] and is described in detail in ref 27. Briefly, following a small polaron transformation,[31] $\hat{H} \rightarrow \hat{\tilde{H}}$, where each $\hat{D}$ operator is renormalized by a corresponding phonon shift operator, e.g., $\hat{D} \rightarrow \hat{D}\hat{X}$ with $\hat{X} = \hat{X}_1^{\dagger}\hat{X}_2$; $\hat{X}_m \equiv \exp[i\lambda_m \hat{P}_{\nu}]$; $\hat{\lambda}_m \equiv V_m^{(\mathrm{e-v})}/\omega_{\nu}$, elastic and inelastic electron currents are obtained using nonequilibrium Green function (NEGF) theory,[32−34] solving using standard approximations coupled equations for electron and phonon Green functions (GFs) and self-energies (SEs), which are needed for current evaluation. The same formalism yields electron and phonon energy currents, and their balance at steady-state determines the junction "effective temperature" according to[30]

$$N_{\nu} \equiv \exp[\omega_{\nu}/T_{\nu} - 1]^{-1} = \frac{\Omega_{\nu} N_{\mathrm{BE}}(\omega_{\nu}) + I_{-}}{\Omega_{\nu} + (I_{+} - I_{-})} \tag{7}$$

where

$$\Omega_{\nu} = 2\pi \sum_{\beta} |U_{\beta}|^2 \delta(\omega_{\nu} - \omega_{\beta})$$

$$N_{\mathrm{BE}}(T, \omega_{\nu}) = \exp[\omega/T - 1]^{-1}$$

and

$$I_{\pm} \equiv \sum_{m=1,2} |V_m^{(\mathrm{e-v})}|^2 \int_{-\infty}^{+\infty} \frac{\mathrm{d}E}{2\pi} G_m^{<}(E) G_m^{>}(E \pm \omega_{\nu})$$

The single electron GFs of the biased junction given in terms of spectral functions associated with the molecule-leads coupling $\Gamma_m^{(K)}(E)$, $m = 1, 2$, $K = L, R$, and the leads Fermi functions $f_K(E)$ by

$$G_m^{<}(E) = i \frac{\Gamma_m^{(L)}(E) f_L(E) + \Gamma_m^{(R)}(E) f_R(E)}{(E - \varepsilon_m)^2 + (\Gamma_m(E)/2)^2}$$

(for $G_m^{>}(E)$ with $if_K(E)$ replaced by $-i(1 - f_K(E))$. It should be noted, however, that the definition of "effective temperature" in a nonequilibrium system is not unique. In particular, how the effective temperatures obtained from different observables compare with each other in nonequilibrium situations is an open question.

Our focus in the present work is the inelastically scattered photon flux. Its calculation requires substantial departure from former methodologies. First, while the electronic nonequilibrium state of the junction is best described within the NEGF formalism, the Raman process with energy-resolved initial and final fluxes is naturally described by scattering theory. A unified description is achieved by considering the molecule as connecting between two "photon baths": an incoming bath with only the incident mode i populated and an outgoing bath that initially has all modes vacant but which can be populated by the scattering off of the molecule.

Another complication arises from the presence of two types of molecule-radiation fields couplings, eqs 6a and 6b. Here we assume that the molecular transition energy $\Delta\varepsilon = \bar{\varepsilon}_2 - \bar{\varepsilon}_1$ and the CT resonances $\bar{\varepsilon}_2 - E_F$, $E_F - \bar{\varepsilon}_1$ are far apart ($\bar{\varepsilon}_m = \varepsilon_m - \lambda_m V_m^{(\mathrm{e-v})}$ are phonon-renormalized electronic energies), and treat their contributions separately. Finally, because Raman scattering is a coherent process, standard approximations used in the analysis of electron-vibration dynamics in inelastic tunneling become inadequate. In particular, the decoupling approximation usually made at the single particle GF level is replaced here by decoupling at what is essentially a two particle GF, yielding the structures of eqs 9−11 below. The procedure is described in detail in ref 27. For the molecular mechanism associated with coupling (6a) it leads to the light scattering flux in the form

$$J_{i \rightarrow f} = J_{i \rightarrow f}^{(\mathrm{nR})} + J_{i \rightarrow f}^{(\mathrm{iR})} + J_{i \rightarrow f}^{(\mathrm{intR})} \tag{8}$$

where

$$J_{i\to f}^{(\mathrm{nR})} = |U_i|^2|U_f|^2 \int_{-\infty}^{+\infty} \mathrm{d}(t-t') \int_{-\infty}^{t} \mathrm{d}t_1 \int_{-\infty}^{t'} \mathrm{d}t_2 \times \mathrm{e}^{-i\nu_i(t_1-t_2)}\, \mathrm{e}^{i\nu_f(t-t')} \langle \hat{X}(t_2)\hat{X}^\dagger(t')\hat{X}(t)\hat{X}^\dagger(t_1)\rangle \times \langle \hat{D}(t_2)\hat{D}^\dagger(t')\hat{D}(t)\hat{D}^\dagger(t_1)\rangle \quad (9)$$

$$J_{i\to f}^{(\mathrm{iR})} = |U_i|^2|U_f|^2 \int_{-\infty}^{+\infty} \mathrm{d}(t-t') \int_{t}^{+\infty} \mathrm{d}t_1 \int_{t'}^{+\infty} \mathrm{d}t_2 \times \mathrm{e}^{-i\nu_i(t_1-t_2)}\, \mathrm{e}^{i\nu_f(t-t')} \langle \hat{X}^\dagger(t')\hat{X}(t_2)\hat{X}^\dagger(t_1)\hat{X}(t)\rangle \times \langle \hat{D}^\dagger(t')\hat{D}(t_2)\hat{D}^\dagger(t_1)\hat{D}(t)\rangle \quad (10)$$

$$J_{i\to f}^{(\mathrm{intR})} = |U_i|^2|U_f|^2 \int_{-\infty}^{+\infty} \mathrm{d}(t-t') \int_{-\infty}^{t} \mathrm{d}t_1 \int_{t'}^{+\infty} \mathrm{d}t_2 \times 2\mathrm{Re}[\mathrm{e}^{-i\nu_i(t_1-t_2)}\, \mathrm{e}^{i\nu_f(t-t')} \langle \hat{X}^\dagger(t')\hat{X}(t_2)\hat{X}(t)\hat{X}^\dagger(t_1)\rangle \times \langle \hat{D}^\dagger(t')\hat{D}(t_2)\hat{D}(t)\hat{D}^\dagger(t_1)\rangle] \quad (11)$$

$J_{i\to f}^{(\mathrm{nR})}$ and $J_{i\to f}^{(\mathrm{iR})}$ describe processes that start and end in the molecular ground and excited states, respectively, "normal" and "inverse" Raman scattering. The third term, eq 11, results from interference between these scattering pathways and is discussed below.

Next, consider the correlation functions in eqs 9−11. Phonon correlation functions such as $\langle \hat{X}^\dagger(t_1)\hat{X}(t_2)\hat{X}(t_3)\hat{X}^\dagger(t_4)\rangle$ can be evaluated by standard methods,[31] that the steady state junction can be associated with an effective thermal distribution, here taken to correspond to the effective temperature (7). The polarization correlation functions, e.g., $\langle \hat{D}^\dagger(t_1)\hat{D}(t_2)\hat{D}(t_3)\hat{D}^\dagger(t_4)\rangle$, are evaluated by invoking two simplifications. First, radiative level broadening is disregarded, and second, energy relaxation due to electron−hole pair creation in the metals is accounted for using the ansatz[35,36]

$$\hat{D}(t) \equiv \mathrm{e}^{i\hat{\bar{H}}t}\hat{D}\mathrm{e}^{-i\hat{\bar{H}}t} \approx \mathrm{e}^{i\hat{\bar{H}}^{(\mathrm{et})}t}\hat{D}\mathrm{e}^{-i\hat{\bar{H}}^{(\mathrm{et})}t}\, \mathrm{e}^{-\Gamma^{(\mathrm{e-h})}t/2} \quad (12)$$

where $\hat{\bar{H}}^{(\mathrm{et})} \equiv \hat{\bar{H}}_0 + \hat{\bar{V}}^{(\mathrm{et})}$ and where[35,36]

$$\Gamma^{(\mathrm{e-h})}(E) = 2\pi \sum_{k_1\neq k_2} |V_{k_1k_2}^{(\mathrm{e-h})}|^2 f_{k_1}[1-f_{k_2}]\delta(E-(\varepsilon_{k_2}-\varepsilon_{k_1})) \quad (13)$$

is the molecular polarization damping rate due to coupling to electron−hole excitations in the leads. Disregarding the energy dependence of $\Gamma^{(\mathrm{e-h})}(E)$, the mixing of levels 1 and 2 due to their interactions with the leads and the effect of electron−phonon interaction on these functions finally leads to

$$\langle \hat{D}(t_2)\hat{D}^\dagger(t')\hat{D}(t)\hat{D}^\dagger(t_1)\rangle \approx \mathrm{e}^{-\Gamma^{(\mathrm{e-h})}(t_1-t+t_2-t')/2} \times [G_1^<(t_1-t_2)G_1^>(t'-t) - G_1^<(t'-t_2)G_1^<(t_1-t)] \times [G_2^>(t_2-t_1)G_2^<(t-t') - G_2^>(t_2-t')G_2^>(t-t_1)] \quad (14)$$

and analogous expressions for the polarization correlation functions that appear in eqs 10 and 11, where $G_m^{>,<}(t)$ ($m = 1, 2$) are the Fourier transform of the junction GFs defined above. Equations 8−14 can now be used to evaluate the Raman scattering flux for our model. Explicit expressions are given in ref 27, and principal results are shown and discussed below.

The mechanism discussed above is expected to dominate the Raman scattering near the molecular resonance. A similar procedure is used in the evaluation of the Raman flask associated with the CT interaction (6b) that can be important for incident frequency near $\bar{\varepsilon}_2 - E_F$ or $E_F - \bar{\varepsilon}_1$.[37,38] For example, the CT analogue of eq 9, the normal Raman scattering associated with metal-to-molecule charge transfer transition that dominates for incident radiation in resonance with this transition, is obtained in the form[27]

$$J_{i\to f}^{(\mathrm{nR})} = \sum_{k,k',k_1,k_2\in\{L,R\}} V_{k_2,i}^{(\mathrm{e-p})}V_{2k',f}^{(\mathrm{e-p})}V_{k2,f}^{(\mathrm{e-p})}V_{2k_1,i}^{(\mathrm{e-p})} \times \int_{-\infty}^{+\infty} \mathrm{d}(t-t') \int_{-\infty}^{t} \mathrm{d}t_1 \int_{-\infty}^{t'} \mathrm{d}t_2 \times \mathrm{e}^{-i\nu_i(t_1-t_2)}\, \mathrm{e}^{i\nu_f(t-t')} \times \langle \hat{X}_2(t_2)\hat{X}_2^\dagger(t')\hat{X}_2(t)\hat{X}_2^\dagger(t_1)\rangle \times \langle \hat{c}_{k_2}^\dagger(t_2)\hat{d}_2(t_2)\hat{d}_2^\dagger(t')\hat{c}_{k'}(t')\hat{c}_k^\dagger(t)\hat{d}_2(t)\hat{d}_2^\dagger(t_1)\hat{c}_{k_1}(t_1)\rangle \quad (15)$$

The nuclear correlation term is evaluated as before. The electronic average is approximated as a product $\langle \hat{c}_{k_2}^\dagger(t_2)\hat{c}_{k'}(t')\hat{c}_k^\dagger(t)\hat{c}_{k_1}(t_1)\rangle \times \langle \hat{d}_2(t_2)\hat{d}_2^\dagger(t')\hat{d}_2(t)\hat{d}_2^\dagger(t_1)\rangle$, and evaluated using Wick's theorem.[27] This again leads to a numerically tractable form.

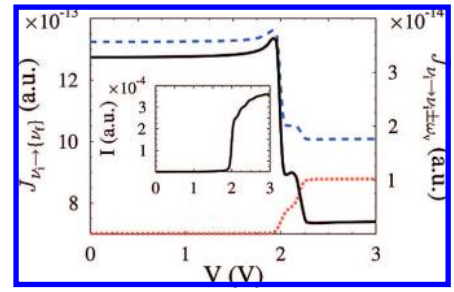

Figure 1. The integrated Raman signal $\bar{J}_{\nu_i\to\{\nu_f\}}$ (solid line, black, left vertical axis), its Stokes $\bar{J}_{\nu_i\to\nu_i-\omega_v}$ (dashed line, blue, right vertical axis) and anti-Stokes $\bar{J}_{\nu_i\to\nu_i+\omega_v}$ (dotted line, red, right) components, and the current I (inset) displayed as functions of the applied bias V. The parameters used are $\nu_i = \bar{\varepsilon}_2 - \bar{\varepsilon}_1$, $E_F = 0$, $\bar{\varepsilon}_1 = -1$ eV, $\bar{\varepsilon}_2 = 1$ eV, $\omega_v = 0.1$ eV, $\Omega_v = 0.005$ eV, $V_1^{(\mathrm{e-v})} = 0.1$ eV, $V_2^{(\mathrm{e-v})} = 0.05$ eV and $T = 100$ K, "a.u." denotes atomic units.

The results shown below are based on the molecular scattering mechanism, eq 6a. (The charge transfer contribution is considered in more detail in ref 27), and demonstrates the main physical results of our theory: the behavior of Raman scattering across the conduction threshold, its applicability for effective temperature determination, and the novel aspects in its interference component.

Figure 1 shows, as functions of biased voltage, the total (elastic and inelastic) scattering flux $\bar{J}_{\nu_i\to\{\nu_f\}}$, as well as its Stokes, $\bar{J}_{\nu_i\to\nu_i-\omega_v}$, and anti-Stokes, $\bar{J}_{\nu_i\to\nu_i+\omega_v}$, components. Here $\bar{J}_{\nu_i\to\nu_f} = \rho_R(\nu_i)\rho_R(\nu_f)J_{i\to f}$, where ρ_R is the density of radiation field modes. The inset shows the current−voltage characteristic, obtained using the procedure of ref 28. A symmetric voltage division factor, i.e., $\mu_K = E_F + \eta_K eV$ ($K = L, R$), $\eta_L = 1 + \eta_R = 0.5$, was used.

At the voltage threshold for conduction (here $V = 2$ V) the molecular levels enter the window between the leads chemical potentials. The current increases accordingly (note its above threshold modulation by the molecular vibration), while the total scattering signal drops by almost half. This can be understood by noting that the total scattering intensity is approximately a sum of the normal and inverse contributions, which, for weak molecule−leads coupling, are proportional to the level population factors $n_1(1 - n_2)$ and $n_2(1 - n_1)$, respectively. Below threshold $n_1 = 1$ and $n_2 = 0$,

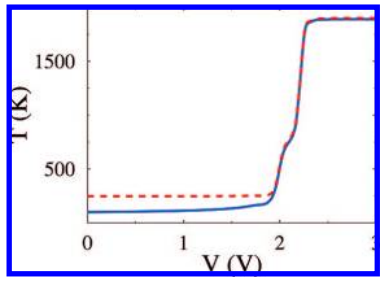

Figure 2. Comparison between the effective vibrational temperature T_v^{eff}, calculated from eq 7 (solid line, blue) and the temperature estimated from the ratio of Stokes and anti-Stokes intensities $T_{\mathrm{S-as}}$, eq 16 (dashed line, red) vs applied bias. Calculation is done for the resonant scattering case $\nu_i = \varepsilon_2 - \varepsilon_1 \equiv \Delta\varepsilon$. Parameters are as in Figure 1 except that $V_1^{(\mathrm{e-v})} = 0.1$ eV and $V_2^{(\mathrm{e-v})} = 0.08$ eV.

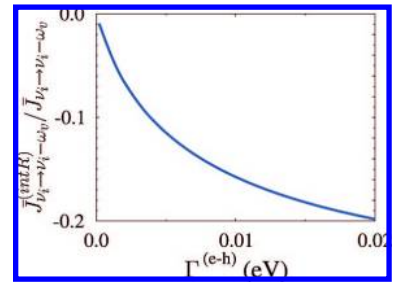

Figure 3. The ratio between the interference component and the total Raman flux at the Stokes frequency, $\bar{J}^{(\mathrm{intR})}_{\nu_i\to\nu_i-\omega_v}/\bar{J}_{\nu_i\to\nu_i-\omega_v}$, at $V = 2.5$ V as a function of $\Gamma^{(\mathrm{e-h})}$ for $\Gamma_m = 0.01$ eV and $\nu_i = \Delta\varepsilon$. Other parameters as in Figure 2.

while well above it $n_1 \approx n_2 \approx 0.5$. The integrated scattering decreases with $n_1(1 - n_2) + n_2(1 - n_1)$. The Stokes intensity similarly decreases; however the anti-Stokes signal increases beyond threshold because of junction heating.

Figure 2 compares the vibrational temperature T of eq 7 to that estimated from the ratio between the Stokes and anti-Stokes Raman components according to

$$T_{\mathrm{S-aS}} = \frac{\omega_v}{\ln\left(\dfrac{\bar{J}_{\nu_i\to\nu_i-\omega_v}(\nu_i+\omega_v)^2}{\bar{J}_{\nu_i\to\nu_i+\omega_v}(\nu_i-\omega_v)^2}\right)} \tag{16}$$

The factors $(\nu_i \pm \omega_v)^2$ correct for the frequency dependence of the outgoing radiation density of modes. The good correspondence seen in Figure 2 indicates the usefulness of both measures. (The apparent deviation of the two measures at low bias results from the inaccuracy in the computed anti-Stokes signal which is extremely small in this voltage regime.) Note, however, that additional frequency-dependent corrections to the S/AS measure may result from resonance structure in the scattering cross section.[26]

Finally, we draw attention to the interesting observation of interference, eq 11, between the two Raman pathways available above the conduction threshold. In a sense, this is a double slit situation, where one path sees the lower (upper) molecular electronic level occupied (empty), while for the other these occupations are interchanged. Interference results from the *correlated* interchange between these pathways, affected by the energy transfer interaction (5) (see Figure 3), which is effective despite the coupling to a *thermal* electronic environment.

In this paper we have outlined a theory of Raman scattering from biased and current-carrying molecular junctions, valid mainly under resonant scattering conditions. The theory makes specific predictions of generic nature that should be observable at and above the conduction threshold: (a) The Stokes component in resonance Raman scattering is predicted to decrease at this threshold, reflecting corresponding changes in molecular level occupations. (b) The anti-Stokes component is predicted to increase, reflecting increase in the molecular temperature above the conduction threshold. (c) The ratio between the Stokes and anti-Stokes intensities can provide a reliable estimate of the junction effective temperature even under the inherently nonequilibrium situation imposed by the voltage bias. Indeed, a first application of Raman scattering for such a temperature estimate has been recently described.[26] One should keep in mind the limitations imposed by our simple model: prediction (a) stems from the assumption that the resonance scattering involves transitions between the molecular HOMO and LUMO. Temperature estimates should take into account signal frequency dependence associated with possible plasmon excitation in the leads. Indeed, the electromagnetic field that enters our calculation is the *local* field that can be obtained for any given junction composition and geometry. With this provision, our conclusions should be valid, at least qualitatively, in many realistic situations.

In addition, we found a new interference component that contributes to the scattered intensity above the conduction threshold. While this contribution to the overall signal cannot be monitored independently, its appearance, resulting from interfering Raman pathways, is interesting and deserves further study.

Junction spectroscopy, in particular Raman scattering, opens new methodological routes for characterization and control of molecular conduction junctions and at the same time provides interesting experimental and theoretical challenges. Future theoretical efforts should focus on extending the theory to better describe the nonresonant scattering regime and on applications to realistic models of molecular junctions.

Acknowledgment. A.N. thanks the US−Israel BSF, ISF, GIF, and ERC for support. M.G. acknowledges the support of UCSD startup funds, UC Academic Senate research grant, and of a LANL Director's Postdoctoral Fellowship. M.R. thanks the Chemistry and MRSEC Divisions of the NSF for support.

References

(1) Flaxer, E.; Sneh, O.; Chesnovsky, O. *Science* **1993**, *262*, 2012.
(2) Wu, S. W.; Ogawa, N.; Ho, W. *Science* **2006**, *312*, 1362.
(3) Katsonis, N.; Kudernac, T.; Walko, M.; van der Molen, S. J.; van Wees, B. J.; Feringa, B. L. *Adv. Mater.* **2006**, *18*, 1397–1400.
(4) Yasutomi, S.; Morita, T.; Imanishi, Y.; Kimura, S. *Science* **2004**, *304*, 1944–1947.
(5) He, J.; Chen, F.; Liddell, P. A.; Andreasson, J.; Straight, S. D.; Gust, D.; Moore, T. A.; Moore, A. L.; Li, J.; Sankey, O. F.; Lindsay, S. M. *Nanotechnology* **2005**, *16*, 695–702.
(6) Li, J.; Speyer, G.; Sankey, O. F. *Phys. Rev. Lett.* **2004**, *93*, 248302.

(7) Kleinekathfer, U.; Li, G.; Welack, S.; Schreiber, M. *Europhys. Lett.* **2006**, *75*, 139–145.
(8) Tikhonov, A.; Coalson, R. D.; Dahnovsky, Y. *J. Chem. Phys.* **2002**, *116*, 10909.
(9) Lehmann, J.; Kohler, S.; May, V.; Hnggi, P. *J. Chem. Phys.* **2004**, *121*, 2278.
(10) Kohler, S.; Lehmann, J.; Hnggi, P. *Phys. Rep.* **2004**, *406*, 379.
(11) Urdaneta, I.; Keller, A.; Atabek, O.; Mujica, V. *J. Phys. B: At. Mol. Opt. Phys.* **2005**, *38*, 3779–3794.
(12) Li, G. Q.; Schreiber, M.; Kleinekathofer, U. *Europhys. Lett.* **2007**, *79*, 27006.
(13) Galperin, M.; Nitzan, A. *J. Chem. Phys.* **2006**, *124*, 234709.
(14) Fainberg, B. D.; Jouravlev, M.; Nitzan, A. *Phys. Rev. B* **2007**, *76*, 245329.
(15) Guhr, D. C.; Rettinger, D.; Boneberg, J.; Erbe, A.; Leiderer, P.; Scheer, E. *Phys. Rev. Lett.* **2007**, *99*, 086801.
(16) Viljas, J. K.; Pauly, F.; Cuevas, J. C. *Phys. Rev. B* **2007**, *76*, 033403.
(17) Jeanmaire, D. L.; VanDuyne, R. *J. Electroanal. Chem.* **1977**, *84*, 1.
(18) Kneipp, K.; Moskovits, M.; Kneipp, H. In *Topics in Applied Physics*; Springer: Berlin and Heidelberg, 2006; Vol. 103.
(19) Nie, S.; Emory, S. R. *Science* **1997**, *275*, 1102.
(20) Kneipp, K.; Wang, Y.; Kneipp, H.; Perelman, L. T.; Itzkan, I.; Dasari, R. R.; Feld, M. S. *Phys. Rev. Lett.* **1997**, *78*, 1667.
(21) Galperin, M.; Ratner, M. A.; Nitzan, A.; Troisi, A. *Science* **2008**, *319*, 1056–1060.
(22) Dadosh, T.; Gordin, Y.; Krahne, R.; Khivrich, I.; Mahalu, D.; Frydman, V.; Sperling, J.; Yacoby, A.; Bar-Joseph, I. *Nature* **2005**, *436*, 677.
(23) Tian, J.-H.; Liu, B.; Li, X.; Yang, Z.-L.; Ren, B.; Wu, S.-T.; Tao, N.; Tian, Z.-Q. *J. Am. Chem. Soc.* **2006**, *128*, 14748–14749.
(24) Ward, D. R.; Grady, N. K.; Levin, C. S.; Halas, N. J.; Wu, Y.; Nordlander, P.; Natelson, D. *Nano Lett.* **2007**, *7*, 1396–1400.
(25) Ward, D. R.; Halas, N. J.; Ciszek, J. W.; Tour, J. M.; Wu, Y.; Nordlander, P.; Natelson, D. *Nano Lett.* **2008**, *8*, 919–924.
(26) Ioffe, Z.; Shamai, T.; Ophir, A.; Cheshnovsky, O.; Selzer, Y. *Nat. Nanotechnol.* **2008**, doi: 10.1038/nnano.2008.304.
(27) Galperin, M.; Ratner, M. A.; Nitzan, A. *arXiv:0808.0292*, 2008.
(28) Galperin, M.; Nitzan, A. *Phys. Rev. Lett.* **2005**, *95*, 206802.
(29) Galperin, M.; Ratner, M. A.; Nitzan, A. *J. Phys.: Condens. Matter* **2007**, *19*, 103201.
(30) Galperin, M.; Nitzan, A.; Ratner, M. A. *Phys. Rev. B* **2007**, *75*, 155312.
(31) Mahan, G. D. *Many-Particle Physics*; Plenum Press: New York, 2000.
(32) Keldysh, L. V. *Sov. Phys. JETP* **1965**, *20*, 1018.
(33) Kadanoff, L. P.; Baym, G. *Quantum Statistical Mechanics*; Frontiers in Physics; W. A. Benjamin, Inc.: New York, 1962.
(34) Haug, H.; Jauho, A.-P. *Quantum Kinetics in Transport and Optics of Semiconductors*; Springer-Verlag: Berlin and Heidelberg 1996; Vol. 123.
(35) Doniach, S. *Phys. Rev. B* **1970**, *2*, 3898.
(36) von Delft, J.; Marquardt, R. A. Florian Smith Ambegaokar V. *Phys. Rev. B* **2007**, *76*, 195332.
(37) Otto, A.; Mrozek, I.; Grabhorn, H.; Akemann, W. *J. Phys.: Condens. Matter* **1992**, *4*, 1143.
(38) Lombardi, J. R.; Birke, R. L.; Lu, T.; Xu, J. *J. Chem. Phys.* **1986**, *84*, 4174–4180.

NL803313F